ISSN 1063-7850, Technical Physics Letters, 2018, Vol. 44, No. 12, pp. 1096–1099. © Pleiades Publishing, Ltd., 2018.
Original Russian Text © A.V. Postnikov, 2018, published in Pis'ma v Zhurnal Tekhnicheskoi Fiziki, 2018, Vol. 44, No. 23, pp. 104–110.

Shock Waves in an Electrochemical Microactuator

A. V. Postnikov

Institute of Physics and Technology (Yaroslavl Branch), Russian Academy of Sciences, Yaroslavl, 150007 Russia
e-mail: mems@yf-ftian.ru

Received July 25, 2018

Abstract—The explosive mode of operation of an electrochemical actuator is studied. In this mode of operation, we observe explosion of microbubbles containing the oxygen–hydrogen gas mixture that forms in the working chamber of the actuator during electrochemical water splitting by high-frequency pulses of alternating polarity. We demonstrate that shock wave emission occurs as a result of implosion of the void formed due to the microbubble explosion, rather than the explosion of the microbubble itself. Using the experimentally measured variation in the bubble wall velocity with the distance from the explosion center, we estimate the pressure amplitude at the shock front. The dynamic of microbubble collapse is established using time-resolved photography.

DOI: 10.1134/S1063785018120337

Membrane-based actuators are widely used in microfluidic technologies [1–3]. They are at the heart of micropumps, valves, and other devices that are used in biological and chemical analyses, drug delivery systems, and sequencing. Performance of these devices is determined by reliability, power consumption, simplicity of design, fabrication costs, biocompatibility, speed of operation, and precision of dosing. Electrochemical actuation is advantageous in that, with a very basic device design, considerable power can be developed. The operation principle of the electrochemical actuator consists in generation of a gas due to an electrochemical reaction, followed by its termination in the system. Long operation cycles due to slow reversal of the gas formation reaction in the actuator's working volume is a major drawback of such an actuator. Operation of electrochemical microactuators based on the water decomposition reaction triggered by applying high-frequency pulses of alternating polarity to produce a gas mixture was demonstrated in [4, 5]. The operation principle of this actuator consists in generation of a hydrogen–oxygen mixture in its working volume. These gases are contained in nanobubbles, which, if a certain level of supersaturation is reached, may coalesce to form microbubbles containing a stoichiometric hydrogen–oxygen mixture. In these microbubbles, the reaction between the hydrogen and the oxygen occurs spontaneously. So far, the factors triggering this reaction have not been fully understood, but the involvement of water nanodroplets was firmly established. The reaction proceeds explosively fast and causes a large pressure buildup in the actuator chamber. In this mode, the operating cycle of the actuator is on the order of a few milliseconds, which is orders of magnitude smaller than the typical operating cycle of currently known devices employed in the microfluidic technology.

In this study, we investigate the performance of the actuator in the explosive regime. The opaque membrane that caps the actuator's working volume, being a hindrance to our measurements, was removed. The device under study attached to a support was placed in a vertical position in a cuvette containing a 1 M sodium sulfate solution. The unfocused beam of a helium–neon laser operating at a wavelength of 632 nm was aligned in line with the electrodes. The beam diameter was 0.55 mm. The beam was deflected horizontally if a gradient of the refraction index appear in the medium. Angular deflection of the beam was transformed into linear displacement in the plane of a photodetector by means of a lens. We used a two-segment photodetector with a bandwidth of 3 MHz. Signals received by both the segments were registered with a PicoScope 5000 digital oscilloscope with an analog bandwidth of 100 MHz. We used a micropositioner that enabled us to set the distance between the device and the laser beam with a precision of 10 μm within a travel range of 50 mm.

Figure 1 shows the stages of the actuator's working cycle: (*1*) generation of a mixture of gases until a certain supersaturation is reached (the incubation period), (*2*) growth of microbubbles, (*3*) a steady state phase, and (*4*) collapse of the microbubbles. Each of the characteristic stages of the operating cycle feature a particular pattern of electric current flowing through the electrolyte. The upper trace in Fig. 1 corresponds to current pulses. The current decay in region *2* lasted for 60–70 μs. The bubble containing the gas mixture enlarged to reach the electrode size, while the current

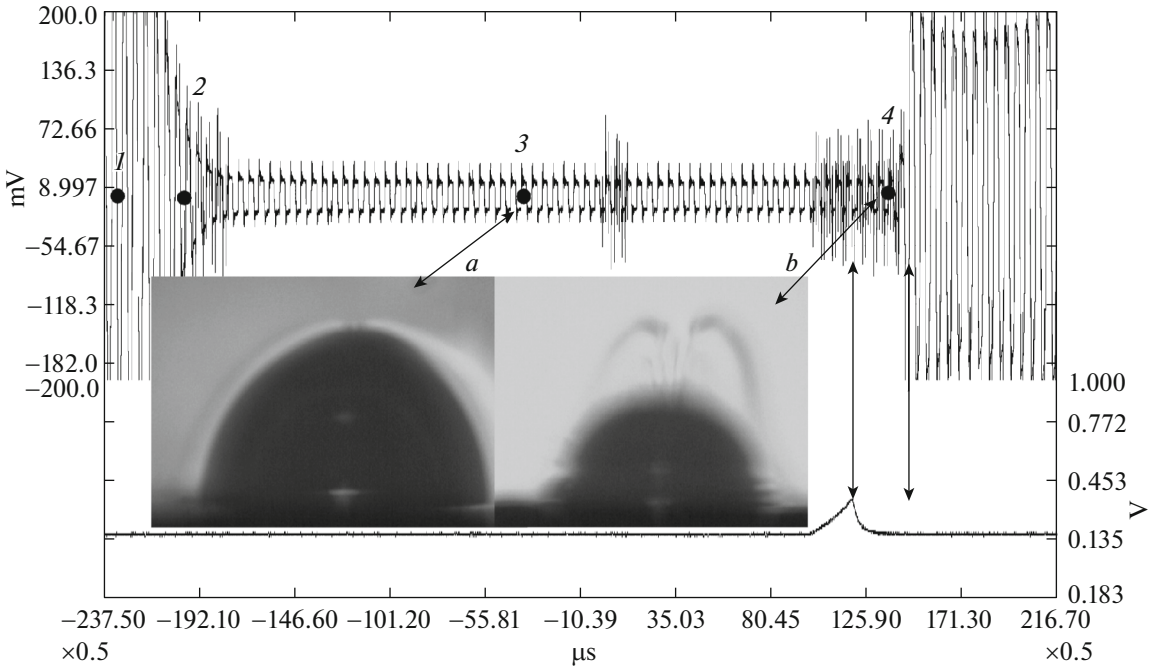

Fig. 1. Scope pattern of the current flowing though the electrolyte and a synchronization pulse of the high-speed camera (regions indicated with numbers *1*–*4* are explained in the text). Inset *a*: shadow image of a bubble in the steady-state phase. Inset *b*: shadow image of a bubble during a synchronization pulse.

drops to nearly zero. That no shock wave emission was observed at this stage can be understood as follows. The liquid over the electrodes becomes saturated with nanobubbles, which form a cloud during the incubation period [6]. The density of this region is less than that of water, and, therefore, it acts as an impact damper, thereby preventing a shock wave from formation. The steady-state phase lasted for 200–300 μs (region *3* in Fig. 1). A shadow image of the bubble (inset *a* in Fig. 1) was taken during this stage. The cloud of nanobubbles can be seen as a bright halo over the bubble in the image. The refraction index in the nanobubble cloud is less than that of the surrounding electrolyte. The bubble was 1.5 mm high. The bubble then collapsed over an ~50-μs (region *4* in Fig. 1), as was established using time-resolved photography. The lower trace in Fig. 1 shows the position of synchronization pulses during which the camera collected the data (exposure, 20 μs). A shadow image shown in inset *b* in Fig. 1 was taken during a synchronization pulse of the camera. The time elapsed between the end of the synchronization pulse and the moment the current was fully re-established was the time required for the bubble implosion (indicated with vertical arrows in Fig. 1). With the bubble collapsed, a shock wave emission occurred. This event produced a gradient in the electrolyte's optical density that was registered by the photodetector. At a short distance from the electrodes, where the wave was generated, the wave velocity exceeded the speed of sound in this media [7]. To measure the shock wave propagation velocity, the laser beam, prior to entering the cuvette, was split into two beams of equal intensity in a horizontal plane by using a birefringent plate. In this way, the wave front first crossed one beam and then the other, the distance between the beam centers being 1.5 mm. Each beam was directed at the two different photodetector segments. By measuring the time between the signal maxima from the two photodetector segments, we can calculate the shock wave propagation velocity, since the distance between the centers of laser beams is known. Signal traces from the photodetector segments are recorded when a shock wave crossed the beams are shown in Fig. 2. The inset shows a broader time interval comprising the signals from the photodetector segments and the corresponding trace of current flowing through the electrolyte during the microbubble birth and then explosion. In Fig. 2, we can see that the end of a signal from segment 1 coincides with the inception of a signal from segment 2. This means that the length of shock wave equals the distance between the laser beams. By knowing the distance separating the beams and the electrodes on the support, one can calculate the variation in the shock wave propagation velocity. Because the distance between the beams is relatively large and wave deceleration occurs within 5–10 mm, these measurements will provide us a lower estimate of the wave velocity. The variation in the shock wave propagation velocity with the distance the wave travelled from the electrodes is shown in Fig. 3. When the distance from electrodes to the middle between the beams exeeds 3 mm, the shock wave velocity equals

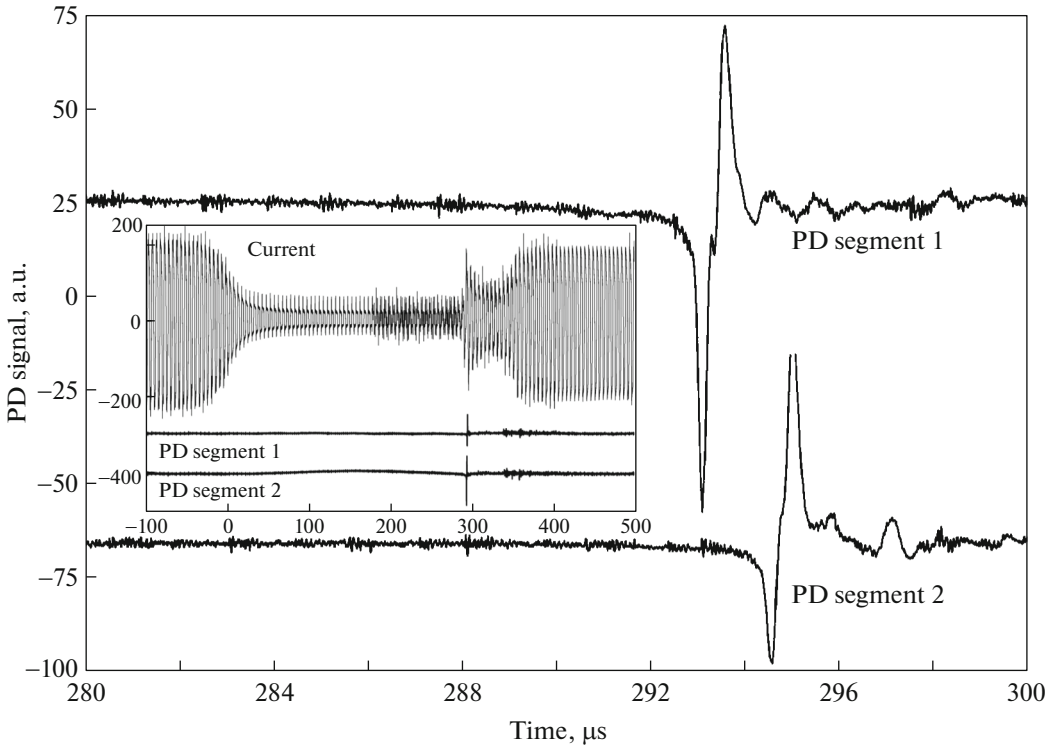

Fig. 2. Signals from the photodiode segments generated when the shock wave crossed the laser beams. Inset: overview scope pattern of the current flowing though the electrolyte.

the speed of sound in the same electrolyte (according to data in [8]). The energy released during the microbubble explosion was not a fixed value and exhibited considerable variation between explosions of different bubbles. After the laser beams were brought within a distance of 1 mm from the electrodes, this variation was especially pronounced (scattering of the experimental data in a broad range). Using the Gilmore model [9] and the Tait equation (an equation of state), the relationship between the pressure and velocity of a shock wave is

$$p_s = (p_a + B)\left(\frac{2nu_s^2}{(n+1)c_0^2} - \frac{n-1}{n+1}\right) - B,$$

where p_s is the shock wave pressure, p_a is the equilibrium pressure in liquid, c_0 is the speed of sound in the electrolyte (1.64 mm/μs), u_s is the shock wave velocity, coefficient n is 7, and constant B is 314 MPa. Using the data shown in Fig. 3, we estimated the pressure amplitude at the shock front, $p_s = 74$ MPa.

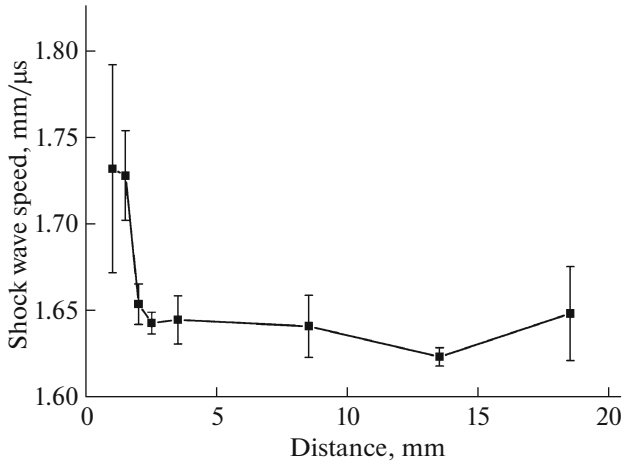

Fig. 3. Variation of the shock wave velocity with the travelled distance.

In summary, in this study, we demonstrated that emission of a shock wave occurs upon collapse of a cavitation bubble that was generated after the explosion of a microbubble containing an oxygen–hydrogen gas mixture. We estimated the shock wave length. Using the Gilmore model and our measurements of the variation in shock wave velocity with the distance traveled by shock wave from source, we also estimated the pressure amplitude at the shock front. The results of this study contribute to development of more deep insight into the processes that take place in electrochemical actuators with an explosive mode of operation.

Acknowledgments. This work was supported by the Federal Agency for Scientific Organizations, Russia. Experiments were performed using equipment of the

Center of Collective Use for characterization of micro- and nanostructures.

REFERENCES

1. Y. Yi, U. Buttner, A. A. A. Carreno, D. Conchouso, and I. G. Foulds, J. Micromech. Microeng. **25**, 105011 (2015).
2. D. E. Lee, S. Soper, and W. Wang, Microsyst. Technol. **14**, 1751 (2008).
3. A. Werber and H. Zappe, J. Microelectromech. Syst. **17**, 1218 (2008).
4. I. V. Uvarov, M. V. Lokhanin, A. V. Postnikov, A. E. Melenev, and V. B. Svetovoy, Sens. Actuators, B **260**, 12 (2018). doi 10.1016/j.snb.2017.12.159
5. V. B. Svetovoy, G. P. Remco, R. G. P. Sanders, and M. C. Elwenspoek, J. Phys.: Condens. Matter **25**, 184002 (2013). doi 10.1088/0953-8984/25/18/184002
6. A. V. Postnikov, I. V. Uvarov, M. V. Lokhanin, and V. B. Svetovoy, PLoS ONE **12**, e0181727 (2017). doi 10.1371/journal.pone.0181727
7. C. E. Brennen, *Cavitation and Bubble Dynamics* (Oxford Univ. Press, New York, Oxford, 1995), p. 282.
8. C. T. Chen, L. S. Chen, and F. J. Millero, J. Acoust. Soc. Am. **63**, 1795 (1978).
9. A. Vogel and S. Busch, J. Acoust. Soc. Am. **100**, 148 (1996).

Translated by A. Kukharuk